ChemComm

FEATURE ARTICLE

View Article Online
View Journal | View Issue

Cite this: *Chem. Commun.*, 2021, **57**, 1080

Mechanochemistry: A force in disguise and conditional effects towards chemical reactions

Srikanth Mateti, †[a] Motilal Mathesh, †[b] Zhen Liu, [c] Tao Tao,[d] Thrinathreddy Ramireddy,[e] Alexey M. Glushenkov,[e] Wenrong Yang *[b] and Ying Ian Chen *[a]

Received 1st October 2020,
Accepted 13th December 2020

DOI: 10.1039/d0cc06581a

rsc.li/chemcomm

Mechanochemistry refers to unusual chemical reactions induced by mechanical energy at room temperatures. It has attracted increased attention because of advantages, such as being a solution-free, energy saving, high-productivity and low-temperature process. However, there is limited understanding of the mechanochemical process because mechanochemistry is often conducted using closed milling devices, which are often regarded as a black box. This feature article shows that mechanochemical reactions can be controlled by varying milling parameters, such as the mechanical force, milling intensity, time and atmosphere. New nanomaterials with doped and functionalized structures can be produced under controlled conditions, which provide a critical insight for understanding mechanochemistry. A fundamental mechanism investigation using force microscopy is discussed.

[a] *Institute for Frontier Materials, Deakin University, Waurn Ponds, Vic 3216, Australia. E-mail: ian.chen@deakin.edu.au*
[b] *School of Life and Environmental Science, Deakin University, Geelong, Victoria 3216, Australia. E-mail: wenrong.yang@deakin.edu.au*
[c] *College of Materials Science and Engineering, Institute for Graphene Applied Technology Innovation, Qingdao University, 308 Ningxia Road, Qingdao 266071, P. R. China*
[d] *School of Materials and Energy, Guangdong University of Technology, Guangzhou 510006, P. R. China*
[e] *Research School of Chemistry, The Australian National University, Canberra, ACT, 2601, Australia*
† These authors contribute equally.

1. Introduction

Mechanical force is known to cause wear and tear due to friction, stress and strain on a large scale, and also at the molecular level, where they can cause chemical reactions in the solid-state by shear stress, breaking symmetry that destabilizes bonds and makes them prone to reaction.[1] In general, chemical reactions take place by energy provided through light, heat or electric potential, and the corresponding fields are termed as photochemistry, thermochemistry and electrochemistry, respectively.[2] Apart from these, it is also possible to activate

Srikanth Mateti

Srikanth Mateti received his PhD degree in 2018 from Deakin University, Australia, and his Master of Technology degree from Jawaharlal Nehru Technological University, Hyderabad, India, in 2011. He has been working as a Research Fellow at the Institute for Frontier Materials (IFM), Deakin University, Australia. His research interests include the in situ synthesis and controlled doping of carbon and nitrogen in various nanomaterials, especially nanotubes (boron nitride, carbon), nanosheets (graphene, BN, etc.) using mechanochemistry (high-energy ball milling), as well as in new applications (thermal management, energy storage and catalysis).

Motilal Mathesh

Motilal Mathesh received his PhD degree (2016) from Deakin University (Australia), in the field of bio-nanotechnology. In 2017, he joined Prof. Daniela Wilson's group at Radboud University (The Netherlands) and was awarded the prestigious Marie Curie Individual fellowship. Recently, he was awarded the Alfred Deakin Postdoctoral Fellowship and joined Deakin University (Australia) as a research fellow. His current research interest focuses on the design and fabrication of 2D nanomotors for biomedical applications.

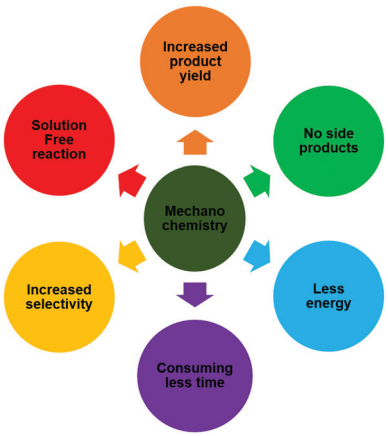

Scheme 1 Advantages of mechanochemistry over solution-based chemistry.

reactions using mechanical force, and this is known as "mechanochemistry", which has a long history and represents mechanically induced chemical reactions.[3–5] Currently, there are various solution-based methodologies used for the synthesis of nanoparticles, such as sol–gel, coprecipitation, microemulsion, sonochemical and ultrasonication.[6] However, all these methods have their limitations in terms of the need for a solvent, which may not be permissible for certain synthesis. In this regard, mechanochemistry is predominantly advantageous for reactions between solids that are not soluble, for reactions in which the use of solvents can interfere or for reactions that are sensitive to the solvent, and for eliminating the need for hazardous solvents in order to make the reactions safer.[7,8] Scheme 1 shows the various features of mechanochemistry that make such reactions far more superior to conventional solution-based methods. Mechanical actions lead to a reduced particle size, production of radicals, creation of active sites or the generation of fresh active surfaces, forming new bonds for chemical reactions to occur.[9]

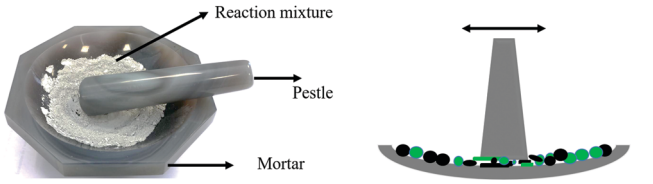

Fig. 1 Traditional method to carry out a chemical reaction with manual grinding.

Traditionally, mortar and pestle (Fig. 1) are common tools used for mechanochemistry; however, the end-product is susceptible to both human and environmental factors depending on the individual force and conditions prevailing during the course of action, thereby making the results unreproducible.[10,11]

In order to circumvent this, with the advent of the industrial revolution, an automated process was introduced called ball milling/grinding, which consists of a closed vessel with ball bearings for carrying out the grinding process, which can be run for longer time periods together with less interference from the surrounding environment.[12] Ball milling instruments can be broadly classified into shakers[13] and planetary mills.[14] In shaker mills, the closed vessels are loaded with ball bearings and shaken at a desired frequency to grind the reagents together. On the other hand, in planetary mills, the jars spin at high speeds in a counter direction to the spinning disc mounted on them. The term planetary is due to the jars revolving around the mounted spinning wheel as the planets revolve around the sun. Recently, the twin-screw extrusion tool was introduced for carrying out mechanochemical reactions and can be considered as an equivalent of solution-based flow reactors for solid-state reactions. In this system, the reagents

Wenrong Yang

Wenrong Yang obtained his PhD degree from the University of New South Wales (UNSW) in 2002. He then worked at CSIRO as a postdoctoral fellow before returning to UNSW in 2005 as a research fellow. He was awarded a University of Sydney Research Fellowship in 2007, and then he joined Deakin University at the end of 2010. He is a Fellow of the Royal Society of Chemistry in the UK, and he currently leads a nanochemistry and biodevices group interested in nanostructured surface chemistry, nanomaterials chemistry, single-molecule electrochemistry and biosensor technology.

Ying Ian Chen

Professor Ying (Ian) Chen received his PhD degree in Chemistry from the University of Paris-Sud, Orsay, France. He worked at the Australian National University, Canberra, for 15 years before moving to Deakin University, Melbourne, in 2009. Professor Chen is the Alfred Deakin Professor, Chair of Nanotechnology, and the Director of a national research centre funded by the Australian Research Council: the ARC Research Hub in New Safe and Reliable Energy Storage and Conversion Technologies, at the Institute of Frontier Materials of Deakin University. He has been working on mechanochemistry and nanotechnology for 25 years and his current research focuses on fundamental research in nanomaterials for energy storage in batteries and fuel cells, environmental protection and medical applications.

are ground with the help of two screws that rotate in opposite directions while being transported through an extrusion barrel.[15] These reactions involve dispersing force and mechanical activation that occur as a statistically probable process according to collision theory.[16] In addition to the different instruments, various grinding techniques have been employed, such as liquid-assisted grinding (LAG),[17] vapour-assisted grinding (VAG),[18] ion and liquid-assisted grinding (ILAG)[19] and polymer-assisted grinding (POLAG),[20] but these will not be discussed here as they are out of the scope of this article.

Mechanochemistry has attracted increasing attention recently because of its application in nanomaterials synthesis.[21] Modern high-energy ball milling can provide sufficient mechanical energy to break the order of the crystalline structure and produce nanometre-scaled crystal seeds. The tiny crystal seeds produced by the mechanical forces can be assembled into large clusters of atoms, which is an effective means for nanostructures growth.[22] Also, the chemical transformation of existing inorganic nanostructures from one material into another can be realized by mechanochemistry at a very low temperature, often at ambient temperature. During the mechanochemical process, the powder particles are repeatedly flattened, cold-welded, fractured and re-welded.[23] Fracture and welding are the two basic events, which produce a permanent exchange of matter between particles and ensure mixing of the various elements of the ground powders. Initially, the particles suffer from very strong high-energy impacts attributed to collisions between the balls themselves and container wall. These strong impacts cause a large amount of microstructural and structural defects in the milled powder particles.[24] The progressive accumulation of defects and the interaction between them lead to crystallite size refinement as well as an increase in the lattice strain. On the other hand, chemical reactions during ball milling occur either gradually or suddenly by mechanically activated combustion. The kinetics of solid-state chemical reactions are ordinarily limited by the rate at which the reactant species can diffuse across the phase boundary, and through the intervening product layers,[25] but the kinetics of mechanochemistry depends on the milling parameters, such as the ball to powder weight ratio, milling speed, milling time[26] and atmosphere, which together allow the control of the mechanochemical processes.

Based on our previous 20 years' research in mechanochemistry, this feature article aims to provide insights regarding different chemical reactions realized by ball milling under different controlled conditions. The effects of mechanical forces on solids both by milling and force microscopy-based mechanochemistry are discussed to aid understanding the difference between thermal and cold mechanical-force-driven reactions. The first section will showcase milling-induced mechanochemistry, and its effects on size and the creation of defect and vacancy sites. This is followed by a description of some new chemical reactions achieved by ball milling both in organic and inorganic chemistry, showing the effect of different milling parameters, such as the milling modes, milling energy, milling time and atmosphere. The next section describes various investigations performed by mechanochemistry using force microscopy, leading up to the final section, which provides the outlook and future perspectives that is desirable to harness the benefits of mechanochemistry to the full extent.

2. Effects of mechanical force on solids

2.1 Milling-induced structural changes

Mechanical action can create irreversible effects on solids due to the strain field produced on them shifting the atoms from the equilibrium position and in some case causes excitation of the electron subsystem,[27] resulting in a metastable state followed by relaxation.[28] Fig. 2 showcases the various defects created in hexagonal boron nitride and graphite by the mechanical action on solids,[29] namely defect accumulation, amorphization and chemical reaction.[30] One of the main factors during milling that imparts such defects is the milling intensity, and mathematically the momentum transfer from the milling process to solids can be described as the product of the impact force and the duration of contact.[31] During this momentum transfer, effects such as wielding, dry friction, plastic shear and fracture take place that give rise to dislocation, grain boundaries, chemical disorder and point defects.[31] We studied the effect of milling conditions on graphite using Raman spectroscopy. A decrease in the I_D/I_G ratio was observed with the increase in the milling time, pointing towards a gradual disordering, while later on the ratio stabilizes, indicating either the force provided by ball milling was not sufficient enough to break the six membered ring or there was a new equilibrium created between the ordering and disordering process.[32]

2.2 Reduction in crystal size

Mechanochemistry can cause a reduction in the crystalline size owing to a strong impact force arising from the milling process. During the milling process, the initial steps are dominated by breaking the crystals and generally require less energy. For instance, a mixture of vanadium oxide and molybdenum oxide (V_2O_5/MoO_3) was ball milled in a planetary mill for 30 to 40 min, resulting in a decrease in the crystalline size of V_2O_5 in the presence of water and the formation of MoV_2O_5 together with a surface coverage of V_2O_5 on MoO_3 upon dry treatment, thus leading to a catalytic behaviour. In both cases, an increase in activity was observed for oxidation reactions, but the latter resulted in higher selectivity towards maleic anhydride formation, a product of the oxidation reaction on *n*-butane.[33]

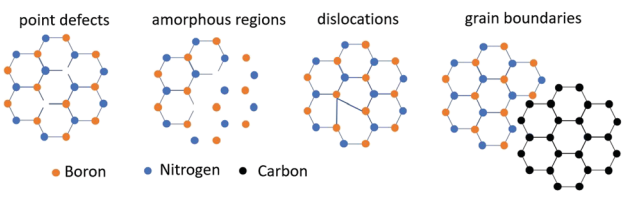

Fig. 2 Defects created by mechanical action on boron nitride.

2.3 Defect formation

Defect formation is the second dominating feature after crystal breaking due to storage of the ball-bearing impact energy as structural defects.[34] Ever since the 1980s, researchers have been keen on studying the effect of mechanical activation on solids with an aim to learn if the defects can lead to new functionality or applications. The vibrational mill can cause strong disorders with electronic defects giving rise to peculiar properties. In one such study oxides such as quartz and zinc ferrite were ball milled to create defects and investigated for the effects on their chemical reactivity. In the case of quartz, the formation of defects helped in better absorption of gases, and the number of molecules adsorbed increased with the increase in amorphization.[35] Similarly, in mechanochemically synthesized zinc ferrite, its sulfur adsorption capacity was observed to increase, induced by microstrains on the structure and the increase in the surface area during high-energy milling.[35]

2.4 Oxidation/vacancy creation

Vacancy creation in solids, especially those of oxygen, can help in realizing potential applications, and such have been reported occurring by mechanochemistry. For instance, the oxidation of brown coal was carried out using ball milling and led to the formation of radicals on the surface of coal. In the presence of H_2O_2, the radicals get oxidized by the formation of phenolic and carboxylic groups, which can act as binding agents for heavy metals. When oxidized, brown coal was used as a sorbent for heavy metal ions in a freshwater body, where no eutrophication was observed, and it further helped phytoplanktons absorb the pollutants.[36] In terms of vacancy creation, magnesium (Mg) was ball milled with cerium oxide (CeO_2) at 120 rpm for 1 h and resulted in improved hydrogen storage.[37] According to the report, ball milling of the above two components resulted in a decrease in Mg domains to nanoscale and also resulted in higher defects at the crystal edges. During hydrogenation, oxygen vacancies were created on CeO_2 due to the transfer of oxygen atoms from CeO_2 to form MgO during ball milling and helped increasing the hydrogen storage capacity.[37]

Mechanical energy can break the chemical bonds in solid materials and produce dangling bonds, which are very active for chemical reactions. In this regard ethanol molecules were observed to produce hydrogen radicals upon interaction with active sites generated in fractured quartz particles.[38] Recently, surprising catalysis was observed on boron nitride even though it is known for its chemical inertness.[39] Consequently, BN nanomaterials with different terminated groups (–OH, $–NH_2$) were tested. Electronic spin resonance (ESR) was used to measure the free radicals and amplitude of the ESR signal, which represents the quantification of radicals in a sample. Fig. 3b shows that only the BN nanoparticle attached with –OH gave a weak ESR signal, due to its spherical shape. Also, 2,2-diphenyl-1-picrylhydrazyl (DPPH) free radicals were quenched by BN nanosheets, and the catalytic activity of these free radicals of BNNSs were analysed by chromogenic reactions of 3,5,3′,5′-tetramethyl benzidine. From UV-Vis spectroscopy (Fig. 3c), it was concluded that boron radicals in BNNSs are active sites for this catalytic behaviour, as witnessed by the strong absorption peak at 520 nm (DPPH showed a violet colour). After the radicals were neutralized on the exposed BNNSs, the colour turned into pale yellow, whereas the absorption peak was shifted for BNQD and BNNS-OH with DPPH, as shown in Fig. 3. It was found that unsaturated boron free radicals on the edges and defect sites on boron nitride nanosheets and nanotubes were key active sites of catalytic behaviour.[40]

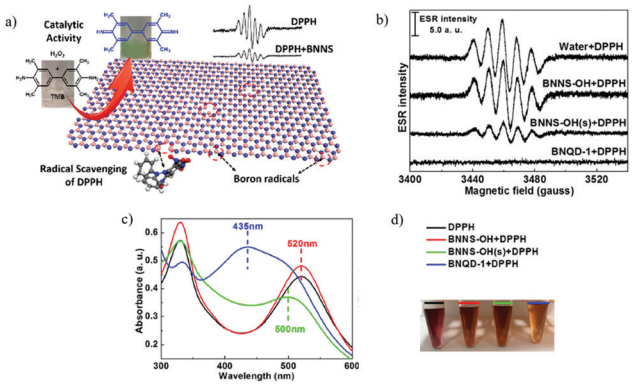

Fig. 3 (a) Radical scavenging method for the detection of boron radicals on BNNSs and the catalytic activity of BNNSs for the oxidation of TMB (b) ESR spectra of DPPH by adding different BN nanomaterials. (c and d) Characterizations of the covalent bonds between DPPH and BNs by UV-vis absorption. (a–d) Reproduced with permission.[39] Copyright 2017, American Chemical Society.

Mechanochemistry can be realized using traditional devices, such as grinders and ball mills. However, new and desired chemical reactions can only take place under certain conditions in terms of milling intensity/energy, frequency, duration, atmosphere and temperature. The effect of these parameters is discussed below.

3. Effect of the milling conditions in mechanochemistry

3.1 Effect of the milling modes: impact or shearing forces

It is important to highlight that the milling mode, especially the nature of the milling action, *i.e.* the presence of either shear, impact forces or a combination of both, has a significant effect on the structure of the nanomaterials in terms of the crystal size and crystallinity and defect level.[41] In the case of Sb, the presence of the sheer force alone did not reduce the size of the particle in the Sb-graphite composite.[42] The structure of the optimal nanocomposite obtained using the milling mode C was visualized by TEM (Fig. 4c). Further, elemental mapping (Fig. 4d) clearly showed that Sb particles with sizes ranging between 5 and 15 nm was dispersed in the carbon matrix. The optimal nanocomposites showed a very stable cyclic behaviour under repeated lithiation and de-lithiation in a lithium-ion battery negative electrode test (Fig. 4e and f).[42] Upon further studies of the preparation conditions, it was established that achieving particle size control (between an average size of ~50 nm and ~1 nm in the corresponding nanocomposites)

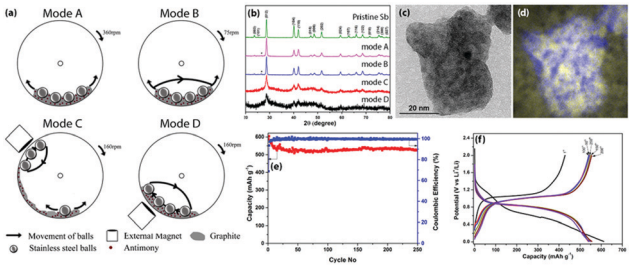

Fig. 4 The preparation, characterization and electrochemical properties of Sb-carbon nanocomposites: (a) schematic illustration of four different milling modes; (b) XRD patterns of the samples milled under these modes; (c and d) energy-filtered TEM images of the optimal nanocomposite milled using mode C (overlay antimony and carbon elemental maps are shown in (d), where the blue colour represents antimony and the yellow colour represents carbon); (e and f) capacity, Coulombic efficiency and charge–discharge profile of the optimal Sb-carbon nanocomposite at a current rate of 230 mA g^{-1}. Adapted with permission.[42] Copyright 2014, Royal Society of Chemistry.

was possible by varying the weight ratio of Sb and graphite between 9 : 1 and 1 : 1 limits during ball milling.[43] The outcomes of these studies illustrate that the structure of the nanocomposites prepared by ball milling depends on the ball milling mode used and the composition of the mixture of the initial precursors. It is important to control these parameters appropriately in the process of nanocomposite fabrication.

3.2 Organic synthesis under different conditions

The earliest example of the use of mechanochemistry for organic synthesis dates back to 1893 for the production of tetrachloroquinhydrone using a mortar and pestle.[44] Mechanochemistry was reinstated again for organic synthesis after 100 years, and since then, various reactions have been successfully performed using mechanochemistry; for instance, it can assist in the formation of carbon–carbon,[45] carbon–heteroatom,[46] metal–ligand coordination bonds,[47] and non-covalent interactions, such as hydrogen bonds or π–π arene stacking interactions.[48] There are various reviews in the literature showcasing all the studied mechanochemistry-based reactions to date; but in here we take only a few examples to show how mechanical force can induce reactions in organic chemistry.

High-speed ball milling (HSBM) is quite commonly used for synthesis in organic chemistry.[49] Here, high-speed vibrations can cause amorphization of the reagents[50] or help in breaking the crystal lattice,[51] which leads to chemical reactions. For instance, the synthesis of phosphorous ylides has been carried out by HSBM, which provides the force to break the crystal lattice of the phosphonium compound to form an amorphous phosphonium salt that undergoes deprotonation in the presence of microcrystalline potassium carbonate (K_2CO_3) in the solid-state reaction. It was also shown that the one-step Witting reaction is possible by ball milling triphenylphosphine, an organic halogenide, and an organic carbonyl compound in the presence of K_2CO_3 (eqn (1)).[51] In the above examples, steel balls were used for ball milling; however, it is also possible to use other metal balls as well that can also act as a catalyst during solid-state reactions. For example, the Sonogashira coupling reaction has been carried out with the help of copper balls instead of steel balls, which not only helped in breaking the crystal lattice for the reaction to occur but also acted as a reaction catalyst that increased the product yield and furthermore allowed easy recovery of the catalyst from the system (eqn (2)).[52] Using mechanical force can also lead to crushing of the catalyst, which gives rise to new active sites that can be further used as active sites for the catalytic reaction.[53] For instance, calcite mineral when crushed gives rise to highly activated naked ionic species that are generated *in situ* and that can act as a strong base capable of deprotonating the active methylene compounds, with the consequent formation of a carbanion stabilized *via* the coordination with calcium cation, which combines with a carbonyl compound, eventually leading to the Knoevenagel product (eqn (3)).[54] The same reaction would not be possible with the use of reagent-grade fine calcite powders as the catalyst, due to the absence of active sites.

Another characteristic feature that is provided by mechanochemistry is bringing molecules into close proximity during milling, which can also give rise to chemical reactions, thereby forming new bonds. Kaupp *et al.* used solvent-free ball milling conditions to synthesize imines[57] and azine (eqn (4))[55] bond based molecules. His group used atomic force microscopy techniques to study the ball-milled products and showed that ball milling results in phase rebuilding and phase transformation upon donating and accepting crystals, such as a hydrazine–hydroquinone complex and benzaldehydes leading to the formation of azines.[55] Ball milling gives rise to certain special conditions, such as a combination of heat, pressure, grinding and stirring, which can help in increasing the product yield, which may not be feasible in solution-based chemistry. For example, nitrones are generally synthesized by the condensation of an aldehyde and hydroxylamines (eqn (5)). Even though good results have been achieved, they have limitations in terms of the need to use organic solvents, the long reaction times, use of an excess of reagents, and the need for tedious chromatographic purifications.[56] These drawbacks could be overcome by the ball milling process, which could also increase the yield of nitrones due to some additional benefits, such as electronic effects or steric constraints on the aldehydes or on the hydroxylamines becoming negligible due to close proximity of the molecules during milling (Fig. 5).[56]

3.3 Effect of the milling time

3.3.1 High-temperature inorganic chemical reactions realized during high-energy ball milling at room temperature. We discovered unusual nitriding reaction sequence during the ball milling of α-Fe in the presence of ammonia, showcasing an increase in milling time complimentarily results in an increase in the nitride phase (eqn (6)).

$$\alpha\text{-Fe} \rightarrow \alpha'\text{-Fe(N)} + \gamma\text{-Fe} \rightarrow \gamma'\text{Fe}_4\text{N} \rightarrow \varepsilon\text{-Fe}_{2-3}\text{N} \quad (6)$$

The nitriding reactions realized by room temperature ball milling go through high-temperature (>590 °C) phase

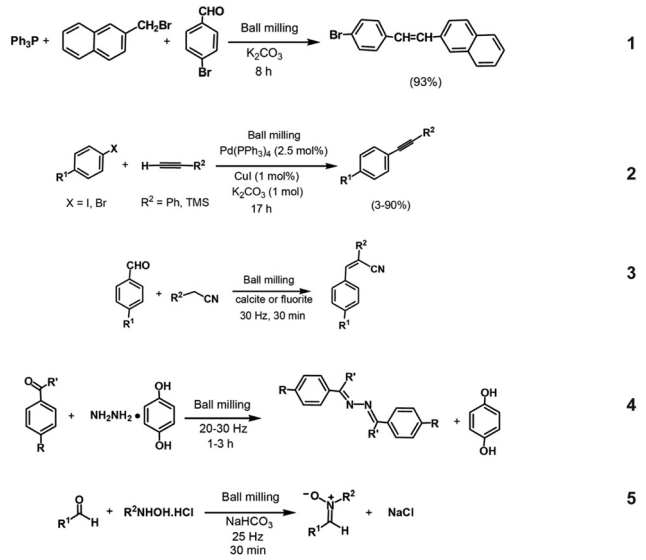

Fig. 5 Various reactions in organic synthesis: (1) one-pot Witting reaction,[51] (2) Sonogashira reaction,[52] (3) Knoevenagal Condensation,[54] (4) azine formation[55] and (5) nitrone synthesis.[56]

transformation in the thermal-equilibrium phase diagram (Fig. 6a), with distinct similarity to nitrogen ion implantation into iron as both result in a good mixing of nitrogen into α-Fe, causing structural rearrangements.[58] The reason why high-temperature reaction sequences can take place at room temperature during ball milling can be explained by the free-energy changes in the Fe–N system, as shown in Fig. 6b. Ball milling increases the free-energy level above the reaction barrier, and so the reactions can occur at room temperature. However, the reaction end-product is still at a high-energy level of E_{Bh} and cannot come to the state E_{Br} because of the low ambient temperature. Therefore, further milling induces a number of reactions/
phase transformations, which normally take place at high temperatures.

3.3.2 Milling-time-dependent reaction sequences. Conventionally, metals exposed to hydrogen gas at certain pressures and temperatures form metal hydrides. These metal hydrides have various applications, such as hydrogen storage and purification.[59] We produced metal hydrides of titanium ($TiH_{1.9}$), zirconium ($ZrH_{1.66}$) and magnesium (MgH_2) using mechanochemistry. The metals were ball milled in the presence of hydrogen gas at room temperature. In a typical experiment, several grams of Ti powder and 20 steel balls (diameter 12 mm) were loaded into the jar and filled with hydrogen gas at 240 kPa. After milling for just 5.5 h, a pressure drop was observed from 240 to −100 kPa (Fig. 7a) indicating, almost all the hydrogen was absorbed into the metals during milling, with subsequent characterizations confirming the formation of metal hydride phases. Hydriding reactions triggered by high-energy impacts during ball milling have a high reaction rate and so this reaction requires only a short period of milling time. This method demonstrates the production of metal hydrides in large quantities in an economical way.[59]

Also, milling-time-dependent nitriding reactions were introduced by milling in an ammonia atmosphere.[63] In a study, Ti was milled in NH_3,[62] in which the gas pressure first decreased from 200 kPa to −100 kPa after just 5 h of milling and then it started to increase during further milling and eventually reached 300 kPa (higher than the starting pressure, 200 kPa) after 120 h of milling, as shown in Fig. 7b. The nitrogen content increased in the metal, whereas the hydrogen content decreased following (Fig. 7c) the below reaction mechanism.

Stage 1: During the early stage of milling (5 h), NH_3 was adsorbed on to the fresh Ti surfaces created by high-energy ball impacts. Then, the adsorbed NH_3 dissociated to H and N;

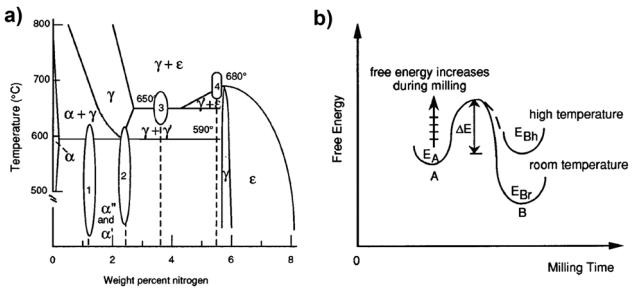

Fig. 6 Nitriding reaction of ball milling anhydrous Fe. (a) Thermal-equilibrium phase diagram of the Fe–N system and (b) schematic of the free-energy changes for ball milled Fe in NH_3.[58] Reproduced with permission.[58] Copyright 1996, American Institute of Physics.

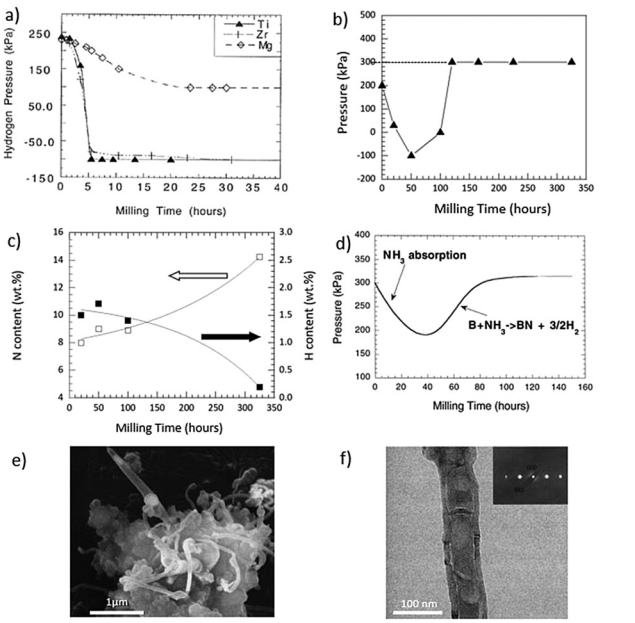

Fig. 7 (a) Variations in hydrogen pressure during the ball milling of Ti, Zr and Mg powders. (b) Variation of pressure with respect to milling time when Ti was milled in NH_3 (c), contents of H and N with respect to the milling time and (d) pressure changes as a function of the milling time during the milling of boron powder in ammonia gas. SEM and TEM images of boron milled for 150 h and an annealed sample (e and f); (a, d–f) Reproduced with permission[59–61] Copyright 2017, Elsevier. (b and c) Reproduced with permission.[62] Copyright 2016, Springer.

thereby forming a layer of TiN, which reacted with H to form $TiH_{1.9}$.

$$Ti + NH_3 \rightarrow TiH_{1.9} + TiN + \text{unreacted Ti} + \text{free surface N}$$

Stage 2: With further extension of the ball milling time, the particle size was further reduced and new surfaces of unreacted Ti reacted with N to form more stable TiN, releasing H_2 gas, which is the reason for the increased pressure after 120 h of milling.

$$TiH_{1.9} + N \rightarrow TiN + H_2$$

A similar reaction sequence was also found in Zr during milling in NH_3.[64] These reaction sequences cannot be realized in a thermal process at high temperature.

The above reaction sequence was discovered in a slow milling process conducted using a slow vertical rotating ball milling with a rotation speed of less than 30 rpm. If a fast and high-energy-milling device is used, *i.e.* a planetary ball mill Fritsch P5, the nitriding reaction can be completed in less than 20 h. Li *et al.* realized the same reaction sequence using a high-energy dielectric barrier discharge plasma-assisted ball mill, which combined ball milling and dielectric barrier discharge plasma.[65] Metals (Mg, Ti) were ball milled in ammonia, with metal hydrides first formed after 6 h of milling and then transformed into nitrides after 16 h of milling. The different reaction kinetics are associated with the different milling intensities.

3.4 Effect of the milling energy

3.4.1 Mechanical activation. Some chemical reactions have a very high activation energy that cannot be supplied by the usual ball milling process and hence, those chemical reactions cannot occur during ball milling. In these cases, ball milling treatment still stores a huge amount of mechanical energy into the treated materials in terms of ensuring a large surface area, high density of defects and intimate mixing between reactants. This substantially reduces the energy barriers, and thus a smaller activation energy is needed to initiate the reactions in thermal processes. For example mechanochemistry has been used to produce one-dimensional boron nitride nanotubes at low temperature.[60] Boron powder was ball milled (for 150 h) in an ammonia atmosphere followed by annealing in a nitrogen atmosphere, producing large amounts of boron nitride nanotubes (BNNTs). Fig. 7d shows the pressure reduction due to gas adsorption in the first 40 h of milling. From 40 to 100 h, the decomposition of ammonia gas takes place due to nitridation reactions between the boron powder and ammonia gas induced by ball milling, with the formation of a B(N) precursor. Subsequent annealing at low temperatures (1000 °C) leads to the formation of BNNTs from the B(N) precursor.[66] Such extensive milling introduces nano-sized metal particles (Fe, Cr, Ni) into B particles. These metal particles also act as a catalyst in the formation of BNNTs (Fig. 7e). The metastable disordered B(N, Fe) nanostructure formed during ball milling and its structural rearrangement during annealing holds the key to understanding the process.

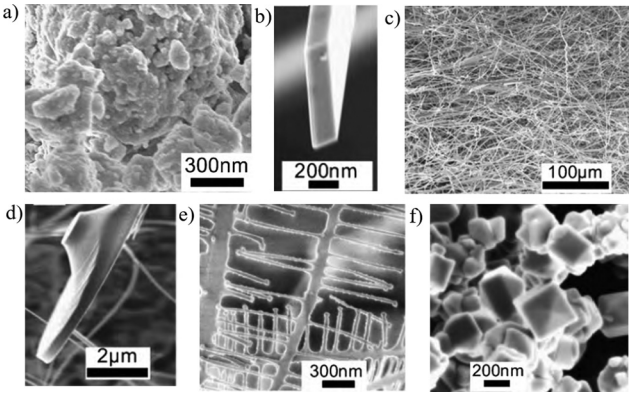

Fig. 8 SEM images of milled and annealed SnO_2; (a) milled sample, (b and c) nanoribbons, (d) nanodiskettes (e) nanobranches, (f) nanoscrystal. Reproduced with permission.[67] Copyright 2017, Elsevier.

In another instance, tin oxide (SnO_2) was milled in an argon atmosphere for 100 h. Various nanostrucures of SnO_2 from the milled samples were synthesized by annealing at a low temperature of 1050–1100 °C.[67] The milled SnO_2 had a reduced particle size with an irregular shape (Fig. 8a). The ball milling process activated the SnO_2 surface, which enabled generating a vapour phase at low temperature, whereas unmilled SnO_2 cannot be vapourised. Nanoribbons (Fig. 8b and c), nanobranches (Fig. 8e), nanodiskettes (Fig. 8d) and nanocrystals (Fig. 8f) were formed based on the vapour condensation process. A similar evaporation behaviour was also observed in milled ZnO,[68] from the evaporation ability generated from the existence of weakly bonded atoms at the grain boundaries, defects and strained areas.

3.4.2 Mechanical exfoliation of nanosheets by low-energy ball milling. Gentle shearing forces created by low-energy ball milling helped in peeling off bulk layered BN into nanosheets in the presence of a liquid exfoliating agent (benzyl benzoate).[69] The starting hBN particles had a diameter sized 0.3–1 μm, as shown in Fig. 9a. The planetary ball mill was loaded with BN and benzyl benzoate. Fig. 9b shows the exfoliated BN nanosheets with the thickness of 2.3–3.7 nm with a conversion yield of 67%. When the high-energy ball milling mode is used, the in-plane structure of the material can be destroyed. Consequently, low-energy milling modes need to be used for nanosheet exfoliation. First, control of the ball rolling actions helped to create a controllable shear force. Second, damage to the in-plane crystal structure was minimized by using small steel balls with a light weight. Third, the use of a liquid exfoliating agent served as a lubricant effect and further reduced strong impact from the balls and gave a gentle shear force. The whole cleavage process can be seen in Fig. 9c–f.[69]

3.5 Effect of the milling atmosphere

The milling atmosphere also has an effect on the material structure. Fig. 10a and b show the XRD patterns of layered graphite and BN milled in different gases. The graphite milled in NH_3 and C_2H_4 maintained its original graphitic structure with reduced diffraction peak intensities, revealing the successful

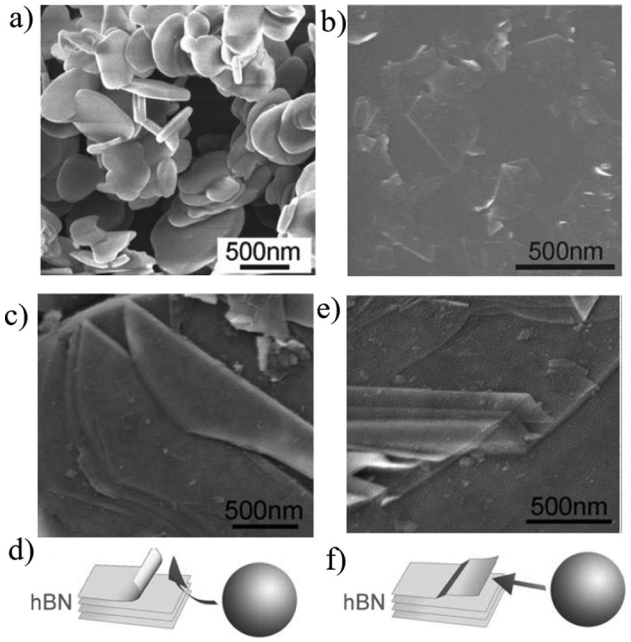

Fig. 9 SEM images of starting hBN particles: (a) exfoliated BN nanosheets (b); SEM images illustrating the exfoliating mechanisms for peeling off and sliding (c and d), rolling over top and shear force. (e and f) thin sheets peeling off the top surface of an hBN. (a–f) Reproduced with permission.[69] Copyright 2017, Royal Society of Chemistry.

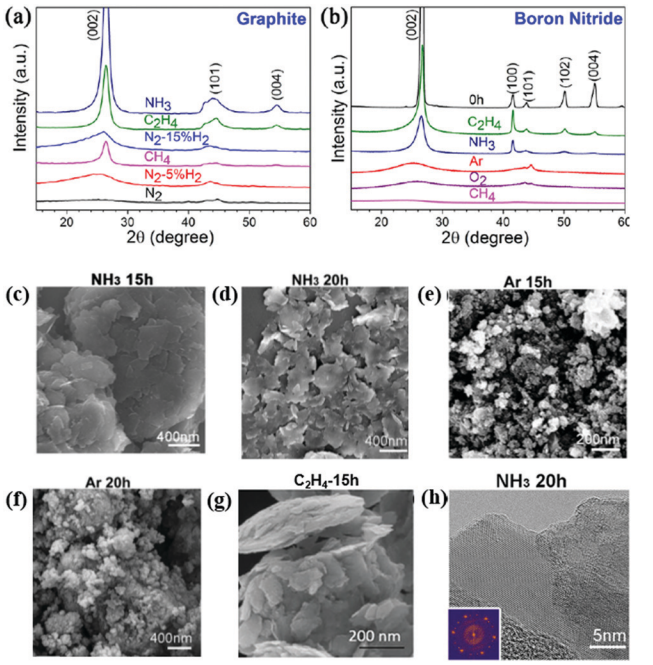

Fig. 10 XRD patterns of graphite (a) and boron nitride (b) milled in different gases for 20 h; SEM images of materials milled in NH_3 atmosphere: (c) graphite, (d) BN; milled in argon atmosphere: (e) graphite, (f) BN. SEM image of MOS_2 milled in C_2H_4 (g) and (h) TEM image of MoS_2 milled in NH_3 atmosphere. (a–f and h) Reproduced with permission[70] Copyright 2016, Springer. (g) Reproduced with permission.[71] Copyright 2015, Royal Society of Chemistry.

exfoliation of graphite (Fig. 10c). On the other hand, graphite milled in N_2, Ar and N_2 + H_2 underwent severe fracturing and plastic deformation under the same milling conditions and became amorphous in structure, as shown in the XRD patterns. A similar behaviour was observed in BN under similar experimental conditions. A sheet-like morphology was observed from the samples milled in NH_3 and C_2H_4, whereas nanometre-sized particles were produced from milling in Ar, O_2 and CH_4 (Fig. 10d and f). This behaviour extended to other 2D materials, such as MoS_2 and WS_2.[70] Pressure reduction was observed in NH_3 and C_2H_4 due to gas adsorption, whereas no pressure reduction was noted in other gases (Fig. 10g and h). The adsorbed gas molecules (NH_3 and C_2H_4) protected the nanosheet structure, and therefore, the layered structure becomes indestructible to high-energy ball impacts.

Two-dimensional (2D) sheets have also been prepared by mechanical cleavage. During mechanical cleavage, the pulling force can easily break the weak van der Waals interaction between layers and leave the strongly sp^2 bonded in-plane structure intact. However, efficient mechanical cleavage while retaining the in-plane crystal structure can only be achieved under suitable mechanochemical conditions. There are several reports on 2D nanomaterials produced by ball milling, where exfoliating agents and surfactants were used to separate the individual layers from bulk layered materials.[72,73] The main disadvantage of using extra agents is the introduction of contaminants, which can affect the properties of the produced nanomaterials. In addition, removing unreacted agents after the synthesis process is time-consuming. Wet milling is a promising method to synthesize large quantities of nanosheets and is a good candidate to enable functionalization and exfoliation in one pot. However, sheets with defects and fragmentation are unavoidable and also, further treatments are required after milling to remove the exfoliation agents used in the wet ball milling process.

Lin *et al.* produced few-layer graphene using different solid exfoliation agents (BN, WC, ZrO and Fe_2O_3) with a plasma-assisted ball mill, and the final graphene layers depended on the agents.[74]

The unique behaviour of layered materials during ball milling in different gases demonstrated not only the indestructible behaviour of the nanosheets but also showed it was a promising method to produce nanosheets in a large quantity and high-quality of graphene, BN, molybdenum disulphide and tungsten disulphide *via* a controlled mechanochemical process.

3.6 Doping and functionalization of nanomaterials

3.6.1 ***In situ*** **doping.** Ball milling in a nitrogen or carbon atmosphere can be used as an efficient and controllable doping technique. For example, N-doped WS_2 nanosheets were produced by the milling of WS_2 in NH_3 as shown by the XRD patterns and SEM images in Fig. 11a and c. There was a gradual increment in nitrogen content in the WS_2 as the milling time increased (Fig. 11b), whereby 8 at% N was found in the milled sample after 100 h of milling showcasing a simultaneous *in situ*

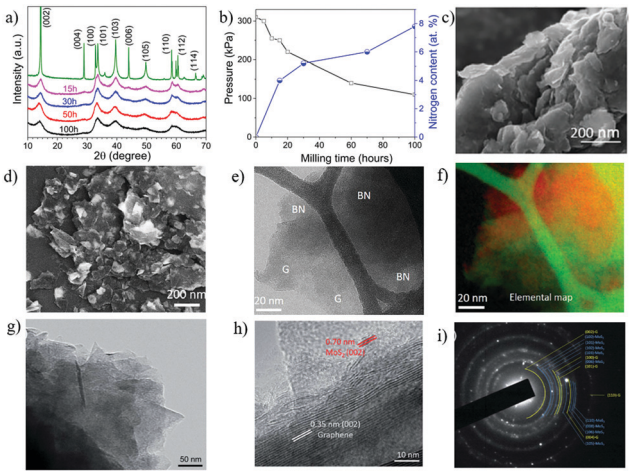

Fig. 11 Structural changes of WS_2 during ball milling in NH_3. XRD patterns (a); nitrogen content in the milled samples as a function of milling time (b), (c) SEM images of the WS_2 sample milled for 15 h in NH_3. (d) SEM images of the graphite and BN composite nanosheets; Energy-filtered TEM (e) an elastic TEM image; (f) an energy-filtered image of the same area with elemental contrast (boron – red, carbon – green); TEM investigation of the MoS_2–G composite nanosheets (20 h) sample: (g) a bright-field TEM image, (h) HRTEM image of the sample; (i) corresponding SAED pattern. (a–c) Reproduced with permission.[71] Copyright 2015, RSC; (d–f) Reproduced with permission.[77] Copyright 2015, Wiley; (g–i) Reproduced with permission[78] Copyright 2017, Wiley.

exfoliation and doping process by the application of mechanical force.[71]

The doping of nitrogen (N) onto the TiO_2 surface has also been carried out for photocatalytic applications under high visible light.[75] The high-energy ball milling of TiO_2 in the presence of ammonium carbonate led to N-doping due to the decomposition of its source hexamethylenetetramine, which gets adsorbed onto the fresh TiO_2 surface produced during the ball milling. Interestingly, it was observed that with an increase in milling time, the photocatalytic activity was reduced due to an increase in the defects and due to amorphization of the crystalline phase. Another notable feature was that the use of zirconia balls for milling resulted in an increase in mechanical energy imparted to TiO_2 when compared to agate balls that have a lower density. Furthermore, with increasing temperature, the highly active anatase was phase transformed to the less active rutile phase, which also led to a decreased photocatalytic activity.[75] Similarly, zinc oxide (ZnO) was also N-doped by ball milling ZnO in the presence of urea, resulting in the intercalation of urea molecules into a crystalline phase of ZnO and leading to its expansion, exhibiting enhanced antibacterial activity upon photoirradiation with visible light.[76]

In addition, hybrid nanosheets can be synthesized with the help of gas exfoliation agent. The ball milling of two powder mixtures (*i.e.* graphite and h BN) in ammonia produce hybrid nanosheets of BN and graphite (Fig. 11d). TEM-EDS analysis confirmed the uniform distribution of BN and G (Fig. 11e and f). Another combination of MoS_2 + graphene hybrid nanosheets was produced by milling in NH_3. The TEM images (Fig. 11g and h) confirmed the sheet-like structure. The SAED patterns (Fig. 11i) revealed a random mixing of nanosheets.

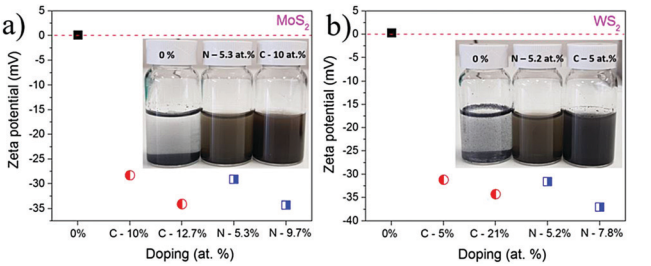

Fig. 12 Zeta potential of samples milled in C_2H_4 and NH_3; MoS_2 (a) and WS_2 (b) Reproduced with permission.[71] Copyright 2015, Royal Society of Chemistry.

Thus, mechanochemistry has become an attractive method for producing various nanostructured materials because of its simplicity, relatively low cost and its applicability to a variety of materials, with one major advantage being its ease to scale up to tonnage quantities of nanostructured material for all kinds of applications.

3.6.2 Functionalization. The ball milling of WS_2 and MoS_2 in NH_3 and C_2H_4 gases results in an *in situ* exfoliation from the bulk material and functionalization of the $-CH_2$ and $-NH_2$ groups on the nanosheets, which helps in the preparation of a stable colloidal dispersion (Fig. 12a and b). Zeta potential measurements showed that pristine MoS_2 and WS_2 dispersions had values of 0.11 and 0.31 mV, respectively, and settled at the bottom of the container. Generally, a stable solution requires a large zeta potential value more than +30 mV or more than −30 mV. Mechanochemical-functionalization treatment achieved a remarkable improvement in the zeta potential values with −34.3 mV for NH-MoS_2 (9.7 at% of N) and −34.1 mV for CH-MoS_2 nanosheets (12.7 at% of C). Similarly, the values were −34.3 and −37 mV for CH- and NH-functionalized WS_2 nanosheets, respectively. A negative potential arises from the functional groups in nanosheets and acts as an anionic surfactant, thereby creating electrostatic repulsion between nanosheets, which in turn helps to stabilize dispersions in water.[71]

Multi-step processes have also been reported. Shao *et al.* used a ball milling method to functionalize black phosphorus (BP) with NH groups. Because urea ($CO(NH_2)_2$) was used as a source of NH, a subsequent washing step was required to remove unreacted urea and unexfoliated BP.[79] Hydrothermal treatment was required for the purpose of activation prior to the ball milling step for the functionalization of MoS_2.[80]

4. Fundamental investigation using force microscopy

The fundamental understanding of mechanochemistry is still limited because of the complicated dynamic milling process. Single-molecule force spectroscopy (SMFS) has been extensively used over the past two decades to study the intermolecular and intramolecular bonding between molecules using mainly atomic force microscopy (AFM). SMFS has revealed the true

and fundamental mechanism of cold mechanical-force driven chemical reactions: breaking bonds and consequent reactions. In the following section, we focus on those. In 1994, SMSF studies were carried out on streptavidin–biotin interactions to observe the molecular level recognition interactions showcasing 3–8 times the difference between specific and non-specific interactions.[81] Later the same year, similar studies were used to determine the adhesive forces between complementary base pairs.[82] With respect to the chemistry world, one of the earliest example was the measurement of the rupture force between Si–C and S–Au bonds that was otherwise not possible,[83] followed by a study of polymers to understand the nanomechanical properties of single polymers,[84] and these have been well discussed in the literature.[85–87] SMSF has been used for studying various chemical and biological phenomena that are discussed below.

4.1 Bond formation

Craig *et al.* used AFM to showcase how mechanical activation can accelerate the nucleophilic substitution of dimethyl sulfoxide for substituted pyridines at square-planar pincer Pd(II) metal centres.[88] This study supported the notions of the stress-free dissociation of Pd(II)–pyridine bonds as occurring by bond-making and breaking components.[88] Following this, the regulation of the chemical reaction by mechanical force was also studied to understand the effect of force on the kinetics of disulfide bond reduction at the single bond level, which cannot be realized by traditional biochemistry.[89] It was observed that disulfide bond reduction could be catalyzed by mechanical force, and the reaction rate was force-dependent.

4.2 Single-molecule delivery

Apart from studying the chemical bonds, AFM has also been utilized to deliver single molecules to surfaces that can be further used for chemical reactions that are very useful for bottom-up technologies. In one such example, reactive polymer molecules attached to one end of the AFM tip were transferred selectively to a modified silicon substrate, where they could be further modified by chemical reactions (Fig. 13a).[90]

4.3 Protein denaturation

Proteins can be denatured easily due to various factors, and hence it is necessary to study the denaturation process in detail in order to prevent its occurrence. SMFS offers a platform to mechanically denature of proteins or to study the effect of force on the reaction rates. Liang and Fernandez, studied the cleavage of the S–S bond using many reducing agents and thioredoxin enzymes. It was observed that the reaction rates of low nucleophiles with S–S bond increased with the applied force, whereas the enzymes exhibited both stretching and resistance favoured reaction rates.[91]

4.4 Nanoscale structure design

With many advancements in technology, nanomachines development has come to the forefront for the fabrication of devices at the nanoscale. This involves the modification of the surfaces at the nanometre scale, which can be achieved by localized chemical reactions. Silicon is one of the most abundantly used elements for electronics due to its semiconductor properties, and hence, they silicon materials need to be modified at the nanoscale for producing miniature devices. One possibility is by protuberance formation on a silicon surface, which can be achieved by sliding a diamond tip on top of the surface, resulting from the concentrated stress that breaks the local Si-Si bonds. The processed part forms SiO_2 and $Si(OH)_4$ due to the presence of oxygen and water on the surface. Upon further carrying out etching using KOH, only the unprocessed part is etched out; thereby resulting in the formation of structures at the nanometre scale.[92] Fig. 13b shows a schematic representation of the above process.[93]

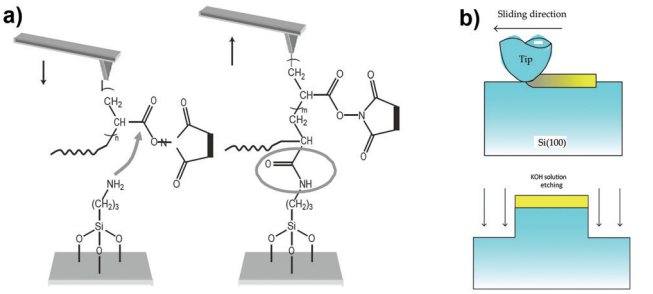

Fig. 13 Mechanochemistry using forced microscopy. (a) During the tip-sample contact, a chemical reaction occurs between the activated esters of a poly-*N*-succinimidyl acrylate chain grafted to the tip and the amino groups of the substrate to form an amide bond, which covalently links the chain to the substrate. (b) Schematic representation for forming nanostructures on silicon using mechanochemical oxidation and then etching using KOH. (a) Reproduced with permission.[90] Copyrights 2006, Nature Publishing Group. (b) Reproduced with permission.[93] Copyrights 2014, Hindawi Publishing Cooperation.

4.5 Polypeptide studies

Single-molecule force spectroscopy has also been employed for the folding and unfolding of polypeptides, which can result in increased or decreased chemical reaction rates. Li *et al.* used AFM to partially unfold a model metalloprotein rubredoxin to expose its FeS_4 centre for studying its reactivity in aqueous solutions. It was demonstrated that exposure of the metal centres causes a destabilization of the FeS_4 centre upon electrophilic protonation and nucleophilic ligand substitution. This was further corroborated by quantum chemistry simulations showing that partial unfolding facilitated the attack on the FeS_4 centre by exogenous ligands in aqueous solutions.[94] Similarly, the protein titin constituting titin kinase (TK) that is present in vertebrate muscle has been studied by AFM for its strain response behaviour. In the folded state, its catalytic activity is blocked due to the presence of a helix blocking the ATP binding site. SMFS was used to selectively remove the helix barrier by mechanical unfolding, which resulted in a successful binding of ATP, thus showcasing TK could act as a biological force sensor.[95]

From a general viewpoint, by using SMFS, researchers can well understand the nanomechanical behaviour of chemical bonds ranging from covalent to non-covalent but still, the

number of studies is limited. We propose a combination of theoretical, experimental, simulation and hands-on experience with mechanical force can help in better understanding and exercising control over chemical reactions.

5. Outlook on the future progression of the field

Further research should be directed towards a better understanding of mechanochemical reactions at the microscopic or molecular levels for its practical implementation and progress, because most of the current highlighted materials lack an appropriate mechanism to elucidate the mechanochemical process.

5.1 Controlling the mechanochemical process *via* crucial parameters is critical for understanding the ball milling process

Controlling the parameters in the mechanochemical process can aid its use and understanding, including the ball to powder ratio, ball-milling speed and milling time milling atmosphere, as they influence the mechanical energy intensity, as well as the energy injection frequency and ambient conditions, which will create chemical reactions, thereby influencing the final product. The milling temperature and atmospheric pressure inside the milling jar are also critical to the thermodynamic reactions of the treated materials. Many current milling instruments do not allow control of these parameters and thus cannot fully control the milling process and end products. The substantial modification of milling devices is required to enable an adjustment of the various parameters. In addition, *in situ* monitoring of the milling process using various detectors allows the establishment of the relationship between the milling conditions and reaction process, providing critical information for understanding the mechanism of the mechanochemical processes. We made possibly the first *in situ* monitored, and instrumented milling device in 1993 based on a vibrating-frame grinder from Fritsch (Fig. 14a).[31] The milling temperature, atmosphere and milling intensity could be changed. The milling impact action was monitored directly using a displacement sensor so that the milling intensity and frequency could be determined, as shown in Fig. 14b. Using this instrument, it was found that Ni_xZr_y compounds become fully amorphized, providing the specific milling intensity was greater than the temperature, *i.e.* the composition-dependent threshold value. Below this threshold, a two-phase structure (crystalline + amorphous) was stabilized. Other milling devices need to be instrumented for monitoring purposes.

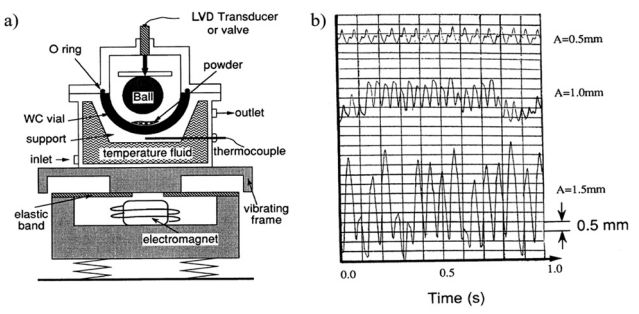

Fig. 14 (a) Scheme of the modified vibrating-frame milling device. (b) Typical records of the movement of the ball relative to the vial, as given by the linear variable differential transformer (LVDT), for vibration amplitudes of the vial: A = 0.5. 1.0 and 1.5 mm, respectively. Reproduced with permission[31] Copyrights 2020, American Physical Society.

The development of new techniques and studying the product formation under fully controlled conditions can help in realizing the desired functionality of nanomaterials. This can also indeed help in increasing the product yield and extending the application of mechanochemistry to a wide range of industries. The temperature of ball mill jars before and after milling has been measured with IR-thermometers or thermocouples. New designs with more *in situ* tools, such as a combination of infrared spectroscopy plus Raman spectroscopy or infrared with X-ray source, would be highly desirable.

5.2 Theoretical studies

Theoretical research is critical to understand new chemistries observed over time. Compared to the large number of reported experimental research studies in mechanochemistry, there is not much theoretical research reported so far. The relationship between the important ball milling parameters and reaction end products has been established through *in situ* monitoring, which has provided important data and new opportunities for theoretical investigation of the mechanochemical processes. The results can be verified using atomic force microscopy, which has been demonstrated to be a powerful tool in understanding the role of mechanical force in molecular changes. Theoretical investigation will provide some pointers for the future direction of mechanochemistry development.

5.3 Green and clean industry process

Mechanochemistry was developed from solid-state chemistry and only expanded into polymer and organic chemistry recently. It has been widely used to synthesize various nanomaterials, and has important industry applications in the preparation of battery materials. The authors and other teams have demonstrated the advantages of it not needing the usage of a solution and it being waste free, but further strong efforts should be made to develop mechanochemistry into green and clear chemical and synthesis processes to replace some current polluting and energy intensive industry processes, which will make a strong contribution to greater environmental protection.

5.4 Scaling up and commercialization of mechanochemistry

Although the traditional ball milling technique has been used by many industries, the modern ball milling technique required for mechanochemistry with controlled energy, atmosphere, temperature and other parameters needs to be scaled up for large-scale applications. Collaboration with industry users is needed to develop large-scale techniques using mechanochemistry that will consume less energy and will be

more efficient. Issuing grading and standardization for different materials is also very important for use in real-life applications. For example, graphene produced from planetary ball mills under certain conditions with specific size should come under one category for certifying the quality.

Conflicts of interest

The authors declare no conflict of interest.

Acknowledgements

M. M. would like to acknowledge Alfred Deakin postdoctoral fellowship from Deakin University for the financial support. Y. C. gratefully thanks the Australian Research Council for the financial support through Discovery and Linkage projects (DP190102656, LP170100784, LE160100199, LP140100608).

References

1 J. J. Gilman, *Science*, 1996, **274**, 65.
2 V. Šepelák, A. Düvel, M. Wilkening, K.-D. Becker and P. Heitjans, *Chem. Soc. Rev.*, 2013, **42**, 7507–7520.
3 G. Heinicke, H.-P. Hennig, E. Linke, U. Steinike, K.-P. Thiessen and K. Meyer, *Cryst. Res. Technol.*, 1984, **19**, 1424.
4 L. Takacs, *Chem. Soc. Rev.*, 2013, **42**, 7649–7659.
5 E. M. Gutman, *Mechanochemistry of Materials*, Cambridge Int Science Publishing, 1998.
6 A. V. Rane, K. Kanny, V. K. Abitha and S. Thomas, in *Synthesis of Inorganic Nanomaterials*, ed. S. Mohan Bhagyaraj, O. S. Oluwafemi, N. Kalarikkal and S. Thomas, Woodhead Publishing, 2018, pp. 121–139.
7 W. Lei, D. Liu and Y. Chen, *Adv. Mater. Interfaces*, 2015, **2**, 1400529.
8 J. L. Howard, Q. Cao and D. L. Browne, *Chem. Sci.*, 2018, **9**, 3080–3094.
9 D. Tan and F. García, *Chem. Soc. Rev.*, 2019, **48**, 2274–2292.
10 J. Andersen and J. Mack, *Green Chem.*, 2018, **20**, 1435–1443.
11 S. L. James, C. J. Adams, C. Bolm, D. Braga, P. Collier, T. Friščić, F. Grepioni, K. D. M. Harris, G. Hyett, W. Jones, A. Krebs, J. Mack, L. Maini, A. G. Orpen, I. P. Parkin, W. C. Shearouse, J. W. Steed and D. C. Waddell, *Chem. Soc. Rev.*, 2012, **41**, 413–447.
12 P. Baláž, M. Achimovičová, M. Baláž, P. Billik, Z. Cherkezova-Zheleva, J. M. Criado, F. Delogu, E. Dutková, E. Gaffet, F. J. Gotor, R. Kumar, I. Mitov, T. Rojac, M. Senna, A. Streletskii and K. Wieczorek-Ciurowa, *Chem. Soc. Rev.*, 2013, **42**, 7571–7637.
13 J. Mack, D. Fulmer, S. Stofel and N. Santos, *Green Chem.*, 2007, **9**, 1041–1043.
14 C. F. Burmeister and A. Kwade, *Chem. Soc. Rev.*, 2013, **42**, 7660–7667.
15 M. Jonoobi, J. Harun, A. P. Mathew and K. Oksman, *Compos. Sci. Technol.*, 2010, **70**, 1742–1747.
16 F. K. Urakaev and V. V. Boldyrev, *Powder Technol.*, 2000, **107**, 93–107.
17 S. Karki, T. Friščić, W. Jones and W. D. S. Motherwell, *Mol. Pharm.*, 2007, **4**, 347–354.
18 M. Đud, O. V. Magdysyuk, D. Margetić and V. Štrukil, *Green Chem.*, 2016, **18**, 2666–2674.
19 T. Friščić, D. G. Reid, I. Halasz, R. S. Stein, R. E. Dinnebier and M. J. Duer, *Angew. Chem., Int. Ed.*, 2010, **49**, 712–715.
20 D. Hasa, G. Schneider Rauber, D. Voinovich and W. Jones, *Angew. Chem., Int. Ed.*, 2015, **127**, 7479–7483.
21 R. Valiev, *Nat. Mater.*, 2004, **3**, 511–516.
22 R. A. Buyanov, V. V. Molchanov and V. V. Boldyrev, *Catal. Today*, 2009, **144**, 212–218.
23 C. Suryanarayana, *Research*, 2019, **2019**, 4219812.
24 T. Xing, S. Mateti, L. H. Li, F. Ma, A. Du, Y. Gogotsi and Y. Chen, *Sci. Rep.*, 2016, **6**, 35532.
25 A. S. Rogachev, *Russ. Chem. Rev.*, 2019, **88**, 875.
26 V. A. Volkov, I. A. El'kin, A. V. Zagainov, A. V. Protasov and E. P. Elsukov, *Phys. Met. Metallogr.*, 2014, **115**, 557–565.
27 P. Y. Butyagin, *Russ. Chem. Rev.*, 1994, **63**, 965–976.
28 I. J. Lin and S. Nadiv, *Mater. Sci. Eng.*, 1979, **39**, 193–209.
29 U. Hoffmann, C. Horst and U. Kunz, in *Integrated Chemical Processes*, ed. K. Sundamacher, A. Kienle and A. Seidel-Morgenstern, Wiley, Weinheim, 2005, pp. 407–436.
30 V. V. Boldyrev and K. Tkáčová, *J. Mater. Synth. Process.*, 2000, **8**, 121–132.
31 Y. Chen, M. Bibole, R. Le Hazif and G. Martin, *Phys. Rev. B: Condens. Matter Mater. Phys.*, 1993, **48**, 14–21.
32 T. Xing, L. H. Li, L. Hou, X. Hu, S. Zhou, R. Peter, M. Petravic and Y. Chen, *Carbon*, 2013, **57**, 515–519.
33 V. A. Zazhigalov, S. V. Khalameida, N. S. Litvin, I. V. Bacherikova, J. Stoch and L. Depero, *Kinet. Catal.*, 2008, **49**, 692–701.
34 A. M. Belenguer, A. A. Michalchuk, G. I. Lampronti and J. K. Sanders, *Beilstein J. Org. Chem.*, 2019, **15**, 1226–1235.
35 U. Steinike and K. Tkáčová, *J. Mater. Synth. Process*, 2000, **8**, 197–203.
36 T. Skripkina, A. Bychkov, V. Tikhova, B. Smolyakov and O. Lomovsky, *Environ. Technol. Inno.*, 2018, **11**, 74–82.
37 P. Liu, H. P. Chen, H. Yu, X. J. Liu, R. Q. Jiang, X. Y. Li and S. X. Zhou, *Int. J. Hydrogen Energy*, 2019, **44**, 13606–13612.
38 F. Delogu, *J. Phys. Chem. C*, 2011, **115**, 21230–21235.
39 Z. Liu, J. Liu, S. Mateti, C. Zhang, Y. Zhang, L. Chen, J. Wang, H. Wang, E. H. Doeven, P. S. Francis, C. J. Barrow, A. Du, Y. Chen and W. Yang, *ACS Nano*, 2019, **13**, 1394–1402.
40 M. Petravic, R. Peter, I. Kavre, L. H. Li, Y. Chen, L.-J. Fan and Y.-W. Yang, *Phys. Chem. Chem. Phys.*, 2010, **12**, 15349–15353.
41 T. Tao, A. M. Glushenkov, C. Zhang, H. Zhang, D. Zhou, Z. Guo, H. K. Liu, Q. Chen, H. Hu and Y. Chen, *J. Mater. Chem.*, 2011, **21**, 9350–9355.
42 T. Ramireddy, M. M. Rahman, T. Xing, Y. Chen and A. M. Glushenkov, *J. Mater. Chem. A*, 2014, **2**, 4282–4291.
43 T. Ramireddy, N. Sharma, T. Xing, Y. Chen, J. Leforestier and A. M. Glushenkov, *ACS Appl. Mater. Interfaces*, 2016, **8**, 30152–30164.
44 A. R. Ling and J. L. Baker, *J. Chem. Soc., Trans.*, 1893, **63**, 1314–1327.
45 M. Jörres, J. L. Aceña, V. A. Soloshonok and C. Bolm, *ChemCatChem*, 2015, **7**, 1265–1269.
46 D. Tan, C. Mottillo, A. D. Katsenis, V. Štrukil and T. Friščić, *Angew. Chem., Int. Ed.*, 2014, **53**, 9321–9324.
47 T. Friščić, in *Ball Milling Towards Green Synthesis: Applications, Projects, Challenges*, ed. A. Stolle and B. Ranu, The Royal Society of Chemistry, UK, 2015, pp. 151–189.
48 G. C. Saunders and T. T. Wehr-Candler, *J. Fluorine Chem.*, 2013, **153**, 162–164.
49 Z. Ze, D. Ya-Wei, W. Guan-Wu and K. Koichi, *Chem. Lett.*, 2004, **33**, 168–169.
50 J. Mack and M. Shumba, *Green Chem.*, 2007, **9**, 328–330.
51 V. P. Balema, J. W. Wiench, M. Pruski and V. K. Pecharsky, *J. Am. Chem. Soc.*, 2002, **124**, 6244–6245.
52 D. A. Fulmer, W. C. Shearouse, S. T. Medonza and J. Mack, *Green Chem.*, 2009, **11**, 1821–1825.
53 V. V. Molchanov and R. A. Buyanov, *Kinet. Catal.*, 2001, **42**, 366–374.
54 S. Wada and H. Suzuki, *Tetrahedron Lett.*, 2003, **44**, 399–401.
55 G. Kaupp and J. Schmeyers, *J. Phys. Org. Chem.*, 2000, **13**, 388–394.
56 E. Colacino, P. Nun, F. M. Colacino, J. Martinez and F. Lamaty, *Tetrahedron*, 2008, **64**, 5569–5576.
57 J. Schmeyers, F. Toda, J. Boy and G. Kaupp, *J. Chem. Soc., Perkin Trans. 2*, 1998, 989–994.
58 Y. Chen, J. S. Williams and G. M. Wang, *J. Appl. Phys.*, 1996, **79**, 3956–3962.
59 Y. Chen and J. Williams, *J. Alloys Compd.*, 1995, **217**, 181–184.
60 Y. Chen, J. F. Gerald, J. Williams and S. Bulcock, *Chem. Phys. Lett.*, 1999, **299**, 260–264.
61 Y. Chen and J. R. Williams, in *Materials Science Forum*, ed. R. Schulz, Trans Tech Publ Ltd, 1996, vol. 225, pp. 881–888.
62 Y. Chen, Z. L. Li and J. S. Williams, *J. Mater. Sci. Lett.*, 1995, **14**, 542–544.
63 Y. Chen, A. Calka, J. Williams and B. Ninham, *Mater. Sci. Eng., A*, 1994, **187**, 51–55.
64 Y. Chen and J. S. Williams, *J. Mater. Res.*, 1996, **11**, 1500–1506.
65 Y. Li, M. Q. Zeng, J. W. Liu and Z. C. Lu, *Ceram. Int.*, 2018, **44**, 18329–18336.
66 J. Yu, Y. Chen, R. G. Elliman and M. Petravic, *Adv. Mater.*, 2006, **18**, 2157–2160.

67 T. Tao, A. M. Glushenkov, H. Hu, Q. Chen and Y. Chen, *J. Alloys Compd.*, 2010, **504**, S315–S318.
68 A. M. Glushenkov, H. Z. Zhang and Y. Chen, *Mater. Lett.*, 2008, **62**, 715–718.
69 L. H. Li, Y. Chen, G. Behan, H. Zhang, M. Petravic and A. M. Glushenkov, *J. Mater. Chem.*, 2011, **21**, 11862–11866.
70 T. Xing, S. Mateti, L. H. Li, F. Ma, A. Du, Y. Gogotsi and Y. Chen, *Sci. Rep.*, 2016, **6**, 1–9.
71 S. Mateti, A. M. Glushenkov, L. H. Li, Q. Ma, C. Zhi and Y. Chen, *Nanoscale Horiz.*, 2019, **4**, 642–646.
72 I.-Y. Jeon, Y.-R. Shin, G.-J. Sohn, H.-J. Choi, S.-Y. Bae, J. Mahmood, S.-M. Jung, J.-M. Seo, M.-J. Kim and D. W. Chang, *Proc. Natl. Acad. Sci. U. S. A.*, 2012, **109**, 5588–5593.
73 I.-Y. Jeon, H.-J. Choi, S.-M. Jung, J.-M. Seo, M.-J. Kim, L. Dai and J.-B. Baek, *J. Am. Chem. Soc.*, 2013, **135**, 1386–1393.
74 C. Lin, L. Yang, L. Ouyang, J. Liu, H. Wang and M. Zhu, *J. Alloys Compd.*, 2017, **728**, 578–584.
75 S. Yin, H. Yamaki, M. Komatsu, Q. Zhang, J. Wang, Q. Tang, F. Saito and T. Sato, *J. Mater. Chem.*, 2003, **13**, 2996–3001.
76 J. Lu, Q. Zhang, J. Wang, F. Saito and M. Uchida, *Powder Technol.*, 2006, **162**, 33–37.
77 Y. Liu, S. Mateti, C. Li, X. Liu, A. M. Glushenkov, D. Liu, L. H. Li, D. Fabijanic and Y. Chen, *Adv. Eng. Mater.*, 2018, **20**, 1700488.
78 S. Mateti, M. M. Rahman, P. Cizek and Y. Chen, *RSC Adv.*, 2020, **10**, 12754–12758.
79 L. Shao, H. Sun, L. Miao, X. Chen, M. Han, J. Sun, S. Liu, L. Li, F. Cheng and J. Chen, *J. Mater. Chem. A*, 2018, **6**, 2494–2499.
80 M. Ahmadi, O. Zabihi, Q. Li, S. M. Fakhrhoseini and M. J. N. Naebe, *Nanomaterials*, 2019, **9**, 1400.
81 G. U. Lee, D. A. Kidwell and R. J. Colton, *Langmuir*, 1994, **10**, 354–357.
82 G. Lee, L. Chrisey and R. Colton, *Science*, 1994, **266**, 771–773.
83 M. Grandbois, M. Beyer, M. Rief, H. Clausen-Schaumann and H. E. Gaub, *Science*, 1999, **283**, 1727–1730.
84 M. Rief, F. Oesterhelt, B. Heymann and H. E. Gaub, *Science*, 1997, **275**, 1295–1297.
85 Y. Bao, Z. L. Luo and S. X. Cui, *Chem. Soc. Rev.*, 2020, **49**, 2799–2827.
86 Y. Liu and G. J. Vancso, *Prog. Polym. Sci.*, 2020, **104**, 15.
87 W. Zhang and X. Zhang, *Prog. Polym. Sci.*, 2003, **28**, 1271–1295.
88 F. R. Kersey, W. C. Yount and S. L. Craig, *J. Am. Chem. Soc.*, 2006, **128**, 3886–3887.
89 A. P. Wiita, S. R. K. Ainavarapu, H. H. Huang and J. M. Fernandez, *Proc. Natl. Acad. Sci. U. S. A.*, 2006, **103**, 7222–7227.
90 A.-S. Duwez, S. Cuenot, C. Jérôme, S. Gabriel, R. Jérôme, S. Rapino and F. Zerbetto, *Nat. Nanotechnol.*, 2006, **1**, 122–125.
91 J. Liang and J. M. Fernández, *ACS Nano*, 2009, **3**, 1628–1645.
92 S. Miyake and J. Kim, *Jpn. J. Appl. Phys.*, 2001, **40**, L1247–L1249.
93 S. Miyake, M. Wang and J. Kim, *J. Nanotechnol.*, 2014, **2014**, 102404.
94 P. Zheng, G. M. Arantes, M. J. Field and H. Li, *Nat. Commun.*, 2015, **6**, 7569.
95 E. M. Puchner, A. Alexandrovich, A. L. Kho, U. Hensen, L. V. Schäfer, B. Brandmeier, F. Gräter, H. Grubmüller, H. E. Gaub and M. Gautel, *Proc. Natl. Acad. Sci. U. S. A.*, 2008, **105**, 13385–13390.